PHOTOSYNTHETICA
International Journal for Photosynthesis Research

DOI 10.32615/ps.2022.011 PHOTOSYNTHETICA 60 (2): 251-258, 2022

Vertical profile of photosynthetic CO_2 response within rice canopy

Y.P. LV+ and Y. PAN

College of Hydraulic Science and Engineering, Yangzhou University, 225009 Yangzhou, Jiangsu, China

Abstract

Leaf-specific Farquhar–von Caemmerer–Berry (FvCB) model was fitted to characterize the vertical profile of photosynthetic CO_2 response within rice canopy. Leaf-position-specific and canopy average FvCB models were fitted to study a suitable leaf representing photosynthetic parameters at the canopy scale. The results showed that leaf photosynthesis was limited by Rubisco activity or ribulose-1,5-bisphosphate regeneration under field conditions. The maximum rate of carboxylation, maximum rate of electron transport, rate of triose phosphates utilization, and light respiration rate in the FvCB model reached the highest values for the top second leaf and then decreased, while the mesophyll diffusion conductance kept decreased in downward leaves. The integrated photosynthetic CO_2-response curves for the top fourth and fifth leaves were appropriate for estimating parameters in the FvCB model at the canopy scale.

Keywords: critical CO_2 concentration; leaf position; parameters in FvCB model.

Introduction

The Farquhar–von Caemmerer–Berry (FvCB) biochemical photosynthetic model has been the heart of estimating crop CO_2 assimilation (Alagarswamy *et al*. 2006, Kattge and Knorr 2007, Zhang *et al*. 2012, Busch *et al*. 2018). Determining the parameters in the FvCB model, namely the maximum rate of carboxylation V_{cmax}, maximum rate of electron transport J_{max}, rate of triose phosphates utilization V_p, mesophyll diffusion conductance g_m, and light respiration rate R_l, is essential to depict the photosynthesis trait by some ecosystem models (Chen *et al*. 1999, Sharkey *et al*. 2007, Patrick *et al*. 2009, Walker *et al*. 2014). Other than reverse calculation (Zhang *et al*. 2014, 2018), fitting leaf photosynthetic CO_2-response (P_N/C_i) curves based on the FvCB model is frequently used to estimate parameters in the FvCB model, which offers a mechanistic way for simulating the photosynthesis from cellular to global

Highlights

- The V_{cmax}, J_{max}, V_p, and R_l reached the highest values for the top second leaf
- The g_m kept decreased in downward leaves
- Top-4th or Top-5th was appropriate for estimating canopy FvCB parameters

Received 14 December 2021
Accepted 23 February 2022
Published online 28 March 2022

+Corresponding author
e-mail: lvyuping@yzu.edu.cn

Abbreviations: C_a – ambient CO_2 concentration; C_{a1} – critical ambient CO_2 concentration for photosynthetic CO_2-response curve at which the transition between Rubisco- and RuBP-limited photosynthesis occurs; C_{a2} – critical ambient CO_2 concentration for photosynthetic CO_2-response curve at which the transition between RuBP- and TPU-limited photosynthesis occurs; C_i – intercellular CO_2 concentration; C_{i1} – critical intercellular CO_2 concentration for photosynthetic CO_2-response curve at which the transition between Rubisco- and RuBP-limited photosynthesis occurs; C_{i2} – critical intercellular CO_2 concentration for photosynthetic CO_2-response curve at which the transition between RuBP- and TPU-limited photosynthesis occurs; FvCB – Farquhar–von Caemmerer–Berry; g_m – mesophyll diffusion conductance; J_{max} – maximum rate of electron transport; P_c – net photosynthetic rates limited by Rubisco activity, P_j – net photosynthetic rates limited by RuBP regeneration; P_N – net photosynthetic rates; P_{N1} – critical net photosynthetic rate for photosynthetic CO_2-response curve at which the transition between Rubisco- and RuBP-limited photosynthesis occurs; P_{N2} – critical net photosynthetic rate for photosynthetic CO_2-response curve at which the transition between RuBP- and TPU-limited photosynthesis occurs; P_N/C_i – photosynthetic CO_2 response; P_p – net photosynthetic rates limited by triose phosphates utilization; R_l – light respiration rate; RuBP – ribulose-1,5-bisphosphate; Top-1st, Top-2nd, Top-3rd, Top-4th, Top-5th, Top-6th, and Top-7th – the top first, second, third, fourth, fifth, sixth, seventh leaf; TPU – triose phosphates utilization; V_{cmax} – the maximum rate of carboxylation; V_p – rate of triose phosphates utilization.

Conflict of interest: The authors declare that they have no conflict of interest.

levels (de Pury and Farquhar 1997, Bernacchi *et al*. 2013, Wu *et al*. 2016, Ren *et al*. 2017).

Leaf photosynthesis is influenced by various leaf attributes, such as leaf chemical elements, specific leaf mass, leaf age, and so on (Pettersen *et al*. 2010, Peri *et al*. 2011, Wang *et al*. 2018, Gong *et al*. 2020). Consequently, the photosynthetic CO_2 response, as well as parameters in the FvCB model, varies greatly among leaves, which has been reported for different crops in different regions (Zhou *et al*. 2007, Yin *et al*. 2009, Qian *et al*. 2012). Moreover, leaf position affects considerably leaf photosynthesis, as the leaves differ in leaf ages and light acclimation within crop canopy (Suzuki *et al*. 2009, Niinemets 2016, Townsend *et al*. 2018). For example, the measured leaf net photosynthetic rates (P_N) at a certain light intensity for wheat decreased significantly in a sequence of the top first, second, third leaf (Li *et al*. 2013). The light-saturated leaf P_N for rice increased to the maximum when a leaf was fully expanded, and then decreased during leaf ontogeny (the upper leaves are physiologically younger than the lower ones), or declined in downward leaves within the canopy (Jin *et al*. 2004, Xu *et al*. 2019, Lv *et al*. 2020). No results were discussing the difference in P_N/C_i curves and parameters in the FvCB model among leaves at different positions. Almost all models treated parameters in FvCB model homogeneously for all rice leaves, that assumed the variation in the P_N was determined by the distribution of both incident irradiance and leaf nitrogen within crop canopy (Kim and Lieth 2003, Greer and Weedon 2011, Wang *et al*. 2021). Insight into the vertical profile of leaf photosynthetic CO_2 response, as well as the parameters in the FvCB model, within the canopy, is critical to understand the vertical characteristic of leaf photosynthesis within crop canopy, which provide basic information to either determine the optional leaf representing canopy photosynthetic parameters, or upscale photosynthesis or photosynthetic parameters from leaf to canopy by considering detailed three-dimensional canopy structure model (Wang *et al*. 2006, Kim *et al*. 2016, Retkute *et al*. 2018).

In the current research, each measured photosynthetic CO_2 response for leaves at different positions was fitted to reveal the vertical profiles of critical CO_2 concentration (at which limited factors of leaf photosynthesis shifted) and parameters in the FvCB model within the rice canopy. Subsequently, leaf-position-specific and canopy average FvCB models were fitted respectively based on measured P_N/C_i curves at each specific position and all P_N/C_i curves within the rice canopy. Finally, the suitable leaf position, at which leaf represented parameters in the FvCB model of rice canopy, was determined by both analyzing the relationship between parameters of leaf-position-specific and canopy average FvCB models and evaluating the performance of canopy average FvCB model in estimating P_N/C_i curves for leaves at different positions.

Materials and methods

Field measurement: The rice (variety of Japonica rice NJ46) was transplanted (13 × 25 cm hill spacing) on 1 July, and harvested on 26 October in 2017 at Kunshan, Jiangsu, East China (31°15'50"N; 120°57'43"E). Primary shoots (about five days after emergence of the top first leaf) under saturated soil moisture content conditions were randomly selected and photosynthetic response to intercellular CO_2 concentration (P_N/C_i) of all leaves on the primary shoot (the top first, second, third, fourth, fifth, sixth, seventh leaf, namely, Top-1st, Top-2nd, Top-3rd, Top-4th, Top-5th, Top-6th, and Top-7th) was measured at 14 ambient CO_2 concentrations (C_a) (in the order of 400, 300, 200, 100, 50, 400, 400, 500, 600, 800; 1,000; 1,300; 1,500; and 1,800 μmol mol^{-1}), by a portable photosynthesis system (*LI-6800*; *LI-COR*, Lincoln, NE, USA) at booting stage. In total, six P_N/C_i curves were measured for leaves at each specific position. For each P_N/C_i curve, photosynthetic photon flux density (PPFD), chamber temperature, and relative humidity were set at 1,600 μmol m^{-2} s^{-1}, 30°C, and 70%, respectively, and such conditions were maintained for 15 min at C_a of 400 μmol mol^{-1} for acclimation and stabilization of leaf photosynthesis before measurements were logged; then leaf P_N was logged automatically at 120-s intervals at each C_a concentration.

FvCB model: The P_N can be estimated according to the steady-state photosynthesis model (Farquhar *et al*. 1980):

$$P_N = \min\{P_c, P_j, P_p\} \quad (1)$$

where P_N [μmol m^{-2} s^{-1}] is net photosynthetic rate at any given chloroplastic CO_2 concentration C_C [μmol mol^{-1}]; P_c, P_j, P_p [μmol m^{-2} s^{-1}] are the P_N limited by Rubisco activity, ribulose-1,5-bisphosphate (RuBP) regeneration, and triose-phosphates utilization TPU, respectively.

$$P_c = \frac{V_{cmax}(C_C - \Gamma^*)}{C_C + K_C\left(1 + \frac{O}{K_O}\right)} - R_l \quad (2)$$

where V_{cmax} [μmol m^{-2} s^{-1}] is the maximal carboxylase activity of Rubisco, R_l [μmol m^{-2} s^{-1}] is the mitochondrial respiration rate, O [210 mmol mol^{-1}] is the oxygen concentration (Manter and Kerrigan 2004), Γ^* [μmol mol^{-1}] is the hypothetical CO_2-compensation point of photosynthesis in the absence of R_l, K_C [μmol mol^{-1}] and K_O [mmol mol^{-1}] are respectively the Michaelis–Menten constant for CO_2 and oxygen.

The parameters of K_C, K_O, Γ^*, R_l at a chamber temperature of 30°C were determined.

$$Parameter = \exp\left(c - \frac{H_a}{R(30 + 237.15)}\right) \quad (3)$$

where *Parameter* is K_C, K_O, Γ^* or R_l; R [8.314 J mol^{-1} K^{-1}] is the molar gas constant, c [dimensionless] and H_a [J mol^{-1}] represent a scaling constant and activation energy, respectively.

$$P_j = \frac{J(C_C - \Gamma^*)}{4C_C + 8\Gamma^*} - R_l \quad (4)$$

where J [μmol m^{-2} s^{-1}] is the rate of photosynthetic electron

transport. J depends on the capacity for photosynthetic electron transport J_{max} [μmol m^{-2} s^{-1}] and PPFD [μmol m^{-2} s^{-1}] according to a nonrectangular hyperbola.

$$J = \frac{\varphi PPFD + J_{max} - \left[\left(\varphi PPFD + J_{max} \right)^2 - 4k\varphi PPFD J_{max} \right]^{1/2}}{2k} \quad (5)$$

where φ [μmol μmol^{-1}] is the initial quantum yield and k [dimensionless] is the curvature of the light response, and parameters of k and φ were 0.3 and 0.90 (Wang *et al.* 2014).

$$P_p = 3V_p - R_l \quad (6)$$

where V_p [μmol m^{-2} s^{-1}] is the rate of TPU.

The C_C and the intercellular CO_2 concentration C_i [μmol mol^{-1}] are related as

$$C_C = C_i - P_N/g_m \quad (7)$$

where g_m [mol m^{-2} s^{-1}] is the mesophyll diffusion conductance from intercellular spaces to chloroplasts.

Generally, the response of P_N to C_i could be described as three phases, namely Rubisco-limited, RuBP-limited, and TPU-limited stage, and the P_N was the minimum of P_c, P_j, and P_p calculated by Eqs. 2, 4, and 6 (Fig. 1). The critical C_i and P_N for each P_N/C_i curve, at which the transitions between Rubisco- and RuBP-limited photosynthesis (C_{i1} and P_{N1}) and between RuBP- and TPU-limited photosynthesis (C_{i2} and P_{N2}) occurred, were determined by deriving the intersection of Eq. 2, Eq. 4 and Eq. 4, Eq. 5 in the FvCB model, respectively. The C_a corresponding with C_{i1} and C_{i2} (C_{a1} and C_{a2}, respectively) were determined by fitting the relationship of C_a with C_i for leaves at each position.

In the current research, each measured P_N/C_i curve was firstly fitted using the nonlinear least-squares regression to determine simultaneously all parameters in the FvCB model, namely V_{cmax}, J_{max}, V_p, R_l, and g_m, which was used to reveal vertical profiles of these parameters within the rice canopy. Moreover, the C_{i1}, C_{a1}, P_{N1}, and C_{i2}, C_{a2}, P_{N2} were determined to reveal the factors that limited photosynthesis for leaves at different positions under various CO_2 concentrations. Furthermore, leaf-position-specific and canopy average FvCB models were fitted respectively based on six measured P_N/C_i curves at each specific position and all P_N/C_i curves within rice canopy. Finally, the suitable leaf position was determined by analyzing the relationship among parameters in leaf-position-specific and canopy average FvCB model and evaluating the performance of canopy average FvCB model in estimating P_N/C_i curves for leaves at different positions.

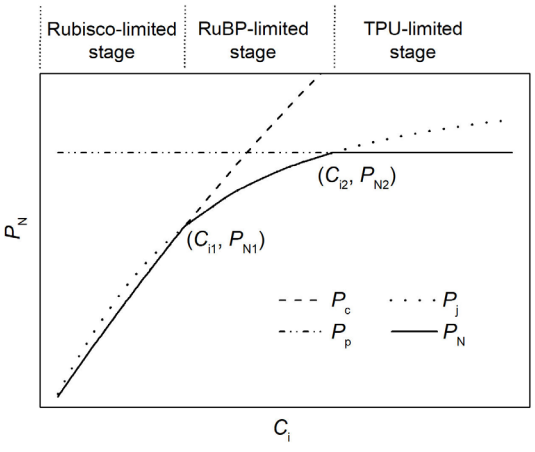

Fig. 1. Fitted response of net photosynthetic rate P_N for rice leaves to intercellular CO_2 concentration C_i based on the FvCB model. The C_{i1}, C_{i2} and P_{N1}, P_{N2} were respectively the critical C_i and P_N at which the transition from Rubisco- to RuBP-limited and from RuBP- to TPU-limited photosynthesis occurred.

Statistical analysis: The one-way analysis of variance (*ANOVA*) and least significant difference multiple comparison tests were used to reveal the differences in C_i and P_N under certain C_a conditions, critical CO_2 concentrations (C_a and C_i), and their corresponding P_N, and parameters in the FvCB model, between leaves at different positions. The performance of leaf-specific, leaf-position-specific, and canopy average FvCB models was evaluated by average absolute error *AE* and the root mean square error *RMSE* (Eqs. 8, 9).

$$AE = \frac{1}{n}\sum_{i=1}^{n}\left|P_{Ncal,i} - P_{Nmea,i}\right| \quad (8)$$

$$RMSE = \sqrt{\frac{1}{n}\sum_{i=1}^{n}\left(P_{Ncal,i} - P_{Nmea,i}\right)^2} \quad (9)$$

where $P_{Ncal,i}$ and $P_{Nmea,i}$ are the P_N estimated by the FvCB model and the corresponding measured value. n is the total number of P_N data.

Results

Measured photosynthetic response to intercellular CO_2 concentration: These P_N/C_i curves were similar among leaves at different positions and could be described as three phases (Fig. 2). As the C_i increased from its minimum concentration, the dP_N/dC_i was high and constant (Rubisco-limited stage), then there was an inflection to a lower dP_N/dC_i that gradually approached zero (RuBP-limited stage). Finally, a further increase in C_i resulted in another transition to a plateau (TPU-limited stage). Furthermore, leaf P_N/C_i curves were quite different from each other between leaves at various positions. Generally, the difference in P_N was small at lower C_i conditions and became more remarkable with increasing C_i. Under the C_i concentration higher than about 350 μmol mol^{-1}, the P_N of the Top-2nd leaf was considerably higher than that of the Top-1st leaf (unfolded and about 5 d after emergence), then gradually declined with a lowering leaf position, and the standard deviation of mean P_N for Top-1st and Top-7th was considerably higher than that for the leaves at the other positions. Especially, the maximum P_N of the Top-2nd was 36.78 μmol m^{-2} s^{-1}, which was 2.76 times the maximum P_N of the Top-7th leaf.

Critical ambient and intercellular CO_2 concentration: The C_i was related linearly with the C_a for leaves at each specific position and the ratio of C_i to C_a (k) decreased to the minimum of 0.624 for the Top-3rd leaf and then increased to the maximum of 0.849 for the Top-7th leaf with downward leaf (Table 1). The three phases of each measured P_N/C_i curve were fitted respectively based on Eq. 2, Eq. 4, and Eq. 6 in the FvCB model. The model performed well in describing P_N/C_i curves, with high R^2 (range from 0.989 to 1.000) and low errors (*RMSE* and *AE* ranged from 0.060 to 1.180 μmol m^{-2} s^{-1} and from 0.041 to 0.781 μmol m^{-2} s^{-1}, respectively). There were differences in C_{i1}, C_{a1}, P_{N1}, and C_{i2}, C_{a2}, P_{N2} between leaves at various positions (Table 1). The C_{i1} for leaves from the Top-2nd to the Top-6th differed slightly (ranging from 345.9 to 399.8 μmol mol^{-1}) and were significantly higher than the Top-1st and Top-7th leaves (270.8 and 264.8 μmol mol^{-1}, respectively). The C_{a1} and P_{N1} reached the maximum for the Top-3rd and Top-2nd leaf (610.8 μmol mol^{-1} and 25.9 μmol m^{-2} s^{-1}), respectively, and then decreased to the minimum for the Top-7th leaf (311.3 μmol mol^{-1} and 6.4 μmol m^{-2} s^{-1}) with lowering leaf position. The C_{i2}, C_{a2}, P_{N2} varied in a wide range of 633.0–988.6 μmol mol^{-1}, 884.6–1291.4 μmol mol^{-1}, 20.3–36.7 μmol m^{-2} s^{-1} for the leaves from the Top-1st to the Top-6th, and the TPU limitation did not occur for the Top-7th leaf. The C_{i2} and C_{a2} increased with lowering leaf position, while the P_{N2} increased at the maximum at the Top-2nd leaf and then decreased with lowering leaf position.

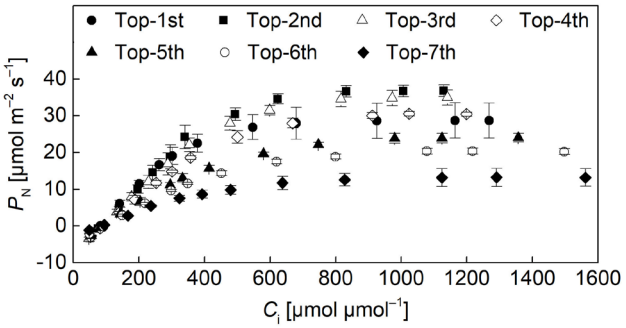

Fig. 2. Measured response of net photosynthetic rate P_N for rice leaves at various positions to intercellular CO_2 concentration C_i. The P_N and C_i denote respectively the mean of six measured leaf P_N and C_i at a certain ambient CO_2 concentration for each specific leaf position, *vertical bars* indicate standard deviation of mean P_N, and Top-1st, Top-2nd, Top-3rd, Top-4th, Top-5th, Top-6th, and Top-7th represent the top first to the top seventh leaf, respectively.

Photosynthetic parameters in the FvCB model: The FvCB model performed well in modeling all individual P_N/C_i curves, and the parameters of V_{cmax}, J_{max}, V_p, R_l, and g_m were considerably different between leaves at various positions (Fig. 3). The V_{cmax}, J_{max}, V_p, and R_l reached the maximum (204.8, 244.3, 14.0, and 5.5 μmol m^{-2} s^{-1}, respectively) for the Top-2nd or Top-3rd leaf, which were significantly higher than that for the Top-1st leaf, and then considerably decreased to the minimum (67.1, 70.1, 7.4, and 1.6 μmol m^{-2} s^{-1}, respectively) for the Top-7th leaf with lowering leaf position. The g_m of 0.3231 mol m^{-2} s^{-1} for the Top-1st leaf was the highest, and the g_m for the Top-2nd to Top-4th leaf (changed insignificantly with the average of 0.2186 mol m^{-2} s^{-1}) was significantly higher than that for the Top-5th to Top-7th leaf (changed insignificantly with the average of 0.1297 mol m^{-2} s^{-1}) with rice canopy.

Leaf-position-specific and canopy average FvCB models: The leaf-position-specific and canopy average FvCB models were fitted respectively for leaves at each specific position and canopy. The parameters of V_{cmax}, J_{max}, V_p, g_m, and R_l varied in a wide range of 57.1–218.6 μmol m^{-2} s^{-1}, 68.5–241.9 μmol m^{-2} s^{-1}, 6.4–15.2 μmol m^{-2} s^{-1}, 0.1344–0.3270 mol m^{-2} s^{-1}, and 1.3–6.1 μmol m^{-2} s^{-1} for the leaf-position-specific FvCB model, and were 157.7 μmol m^{-2} s^{-1}, 167.3 μmol m^{-2} s^{-1}, 9.7 μmol m^{-2} s^{-1}, 0.1347 mmol m^{-2} s^{-1}, and 3.4 μmol m^{-2} s^{-1} for the canopy-average FvCB model (Table 2). Generally, the parameters in the

Table 1. The linear relationship of intercellular CO_2 concentration C_i with ambient CO_2 concentration C_a, and the critical C_i, C_a and net photosynthetic rate P_N at which the transition from Rubisco- to RuBP-limited (C_{i1}, C_{a1}, P_{N1}, respectively) and from RuBP- to TPU-limited (C_{i2}, C_{a2}, P_{N2}, respectively) photosynthesis occurred for leaves at different positions. Top-1st, Top-2nd, Top-3rd, Top-4th, Top-5th, Top-6th, and Top-7th – the top first to the top seventh leaf, respectively; k – the ratio of C_i to C_a; R^2 – coefficient of determination for $C_i = kC_a$. Data in row of C_{i1}, C_{a1}, P_{N1}, C_{i2}, C_{a2}, and P_{N2} denote 'average ± standard deviation', and the average is the mean of six derived C_i, C_a or P_N at specific leaf position. *Different letters* represent significant difference in C_{i1}, C_{a1}, P_{N1}, C_{i2}, C_{a2} or P_{N2} between leaves at different positions at $p<0.05$.

Leaf position	$C_i = kC_a$	R^2	C_{i1} [μmol mol^{-1}]	C_{a1} [μmol mol^{-1}]	P_{N1} [μmol m^{-2} s^{-1}]	C_{i2} [μmol mol^{-1}]	C_{a2} [μmol mol^{-1}]	P_{N2} [μmol m^{-2} s^{-1}]
Top-1st	$C_i = 0.710C_a$	0.982	270.8 ± 29.8^{a}	378.5 ± 41.6^{ab}	17.8 ± 3.9^{a}	633.0 ± 137.4^{a}	884.6 ± 192.0^{a}	28.7 ± 4.8^{a}
Top-2nd	$C_i = 0.635C_a$	0.991	379.5 ± 60.4^{b}	595.3 ± 94.8^{c}	25.9 ± 2.5^{b}	717.6 ± 71.5^{ab}	1,125.7 ± 112.1^{b}	36.7 ± 1.5^{b}
Top-3rd	$C_i = 0.624C_a$	0.993	382.3 ± 73.7^{b}	610.8 ± 117.8^{c}	23.9 ± 4.1^{bc}	754.5 ± 76.5^{b}	1,205.4 ± 122.2^{bc}	34.8 ± 2.1^{b}
Top-4th	$C_i = 0.668C_a$	0.991	399.8 ± 49.0^{b}	596.8 ± 73.2^{c}	21.1 ± 3.1^{ac}	865.2 ± 91.3^{c}	1,291.4 ± 136.3^{c}	30.4 ± 0.5^{a}
Top-5th	$C_i = 0.745C_a$	0.995	345.9 ± 54.6^{b}	463.7 ± 73.2^{b}	13.8 ± 2.3^{d}	954.5 ± 73.8^{cd}	1,279.7 ± 99.0^{c}	23.9 ± 1.3^{c}
Top-6th	$C_i = 0.809C_a$	0.996	357.3 ± 21.0^{b}	441.0 ± 25.9^{b}	12.2 ± 1.3^{d}	988.6 ± 9.1^{d}	1,220.3 ± 11.2^{bc}	20.3 ± 0.8^{d}
Top-7th	$C_i = 0.849C_a$	0.996	264.8 ± 63.3^{a}	311.3 ± 74.4^{a}	6.4 ± 2.6^{e}	-	-	-

FvCB model of the Top-4th or Top-5th were near to these parameters in the canopy-average FvCB model, which indicated that the Top-4th or Top-5th represented the photosynthetic parameters of rice canopy.

The leaf-position-specific FvCB model performed much better than the canopy-average FvCB model in estimating leaf P_N (Fig. 4). For leaves at different positions, the estimated P_N based on leaf-position-specific FvCB model accounted for 97.8–99.9% of measured P_N with R^2, *RMSE*, and *AE* of 0.978–0.999, 0.613–2.767 μmol m^{-2} s^{-1}, and 0.448–2.055 μmol m^{-2} s^{-1}, while the estimated P_N based on canopy average FvCB model accounted for 70.0–197.9% of measured P_N with R^2, *RMSE*, and *AE* of 0.902–0.997, 2.488–9.555 μmol m^{-2} s^{-1}, and 1.901–8.371 μmol m^{-2} s^{-1} (Fig. 4*A–G*). For all leaves within the canopy, the estimated P_N based on the leaf-position-specific FvCB model accounted for 99.4% of measured P_N with R^2, *RMSE*, and *AE* of 0.994, 1.472 μmol m^{-2} s^{-1}, and 0.962 μmol m^{-2} s^{-1}, while the estimated P_N based on the canopy-average FvCB model accounted for 90.2% of measured P_N with R^2, *RMSE*, and *AE* of 0.902, 5.750 μmol m^{-2} s^{-1}, and 4.426 μmol m^{-2} s^{-1} (Fig. 4*H*). Generally, the leaf-position-specific FvCB model performed well in estimating P_N for all leaves at different positions, and the canopy average FvCB model underestimated P_N for the top four leaves and overestimated P_N for the other leaves lower than the Top-4th. While the canopy-average FvCB model performed well in estimating mixed P_N from the Top-4th and Top-5th leaves, and the estimated P_N accounted for 98.0% of measured P_N with R^2, *RMSE*, and *AE* of 0.979, 2.521 μmol m^{-2} s^{-1}, and 2.034 μmol m^{-2} s^{-1} (Fig. 4*I*), which meant the integrated P_N/C_i curves for the Top-4th and Top-5th were appropriate for estimating photosynthetic parameters at canopy scale.

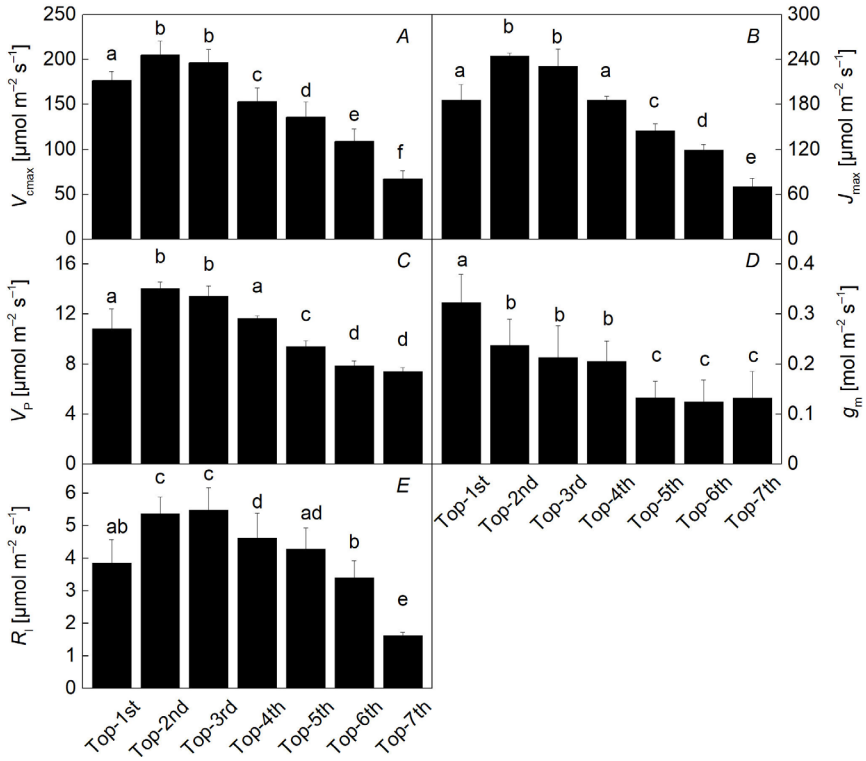

Fig. 3. The mean of leaf specific maximum rate of carboxylation V_{cmax} (*A*), maximum rate of electron transport J_{max} (*B*), rate of triose phosphates utilization V_p (*C*), mesophyll diffusion conductance g_m (*D*), and light respiration rate R_l (*E*) at specific leaf position within rice canopy. Columns denote the mean of six parameters in FvCB model calibrated based on measured each leaf photosynthetic CO_2-response curves at specific leaf position, *bars* show the standard error of the mean, and Top-1st, Top-2nd, Top-3rd, Top-4th, Top-5th, Top-6th, and Top-7th represent the top first to the top seventh leaf, respectively.

Table 2. The maximum rate of carboxylation (V_{cmax}), maximum rate of electron transport (J_{max}), rate of triose phosphates utilization (V_p), light respiration rate (R_l), and mesophyll diffusion conductance (g_m) in leaf-position-specific and canopy average FvCB models. Top-1st, Top-2nd, Top-3rd, Top-4th, Top-5th, Top-6th, Top-7th – the top first to the top seventh leaf, respectively.

Parameter	Leaf-position-specific FvCB							Canopy average FvCB
	Top-1st	Top-2nd	Top-3rd	Top-4th	Top-5th	Top-6th	Top-7th	
V_{cmax} [μmol m^{-2} s^{-1}]	177.3	215.5	218.6	157.1	114.3	84.9	57.1	157.7
J_{max} [μmol m^{-2} s^{-1}]	186.8	241.9	240.9	190.9	136.8	108.4	68.5	167.3
V_p [μmol m^{-2} s^{-1}]	10.8	14.2	13.6	11.7	15.2	15.2	6.4	9.7
R_l [μmol m^{-2} s^{-1}]	3.9	5.8	6.1	4.7	3.6	2.6	1.3	3.4
g_m [mol m^{-2} s^{-1}]	0.3270	0.2173	0.1763	0.1822	0.1646	0.1911	0.1344	0.1347

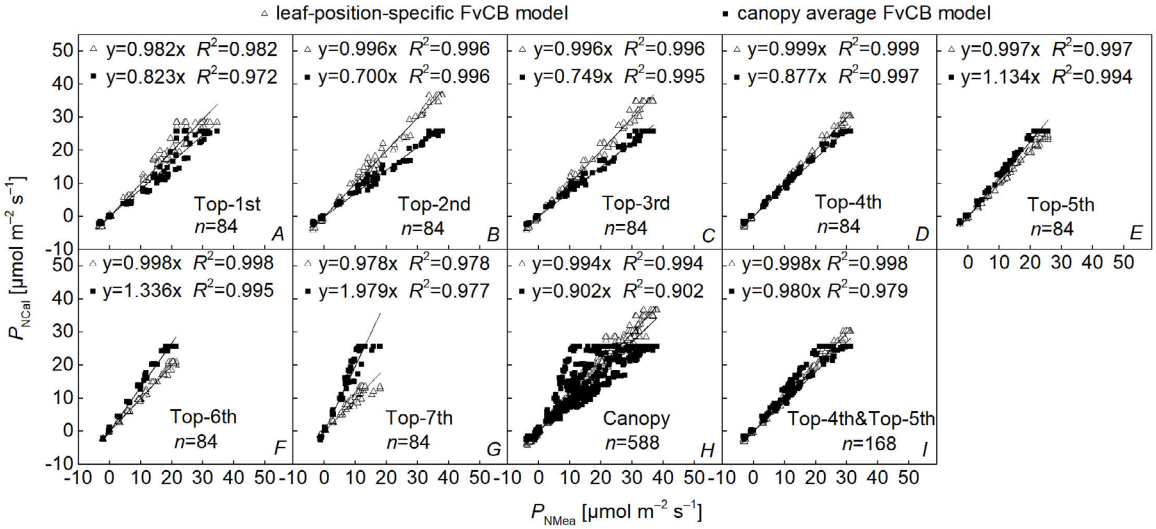

Fig. 4. Linear regression of measured photosynthetic rate P_{NMea} with estimated photosynthetic rate P_{NCal} based on leaf-position-specific and canopy average FvCB model. Top-1st, Top-2nd, Top-3rd, Top-4th, Top-5th, Top-6th, and Top-7th represent the top first to the top seventh leaf, respectively, and n is the total number of P_{NMea} data.

Discussion

The P_N initially increased linearly with the increase in C_i, then slowly up to the maximum, and kept at a steady state (Fig. 2), which was consistent with the previous reports (Sharkey *et al*. 2007). The P_N at a certain C_i reached the maximum for the Top-2nd leaf and gradually declined with lowering leaf position (Fig. 2). Similarly, Wang *et al*. (2009) showed that the P_N at PPFD of 1,200 μmol m^{-2} s^{-1} reached the highest value at the last second leaf and then decreased gradually in downward leaves at the tillering stage (9-leaf stage correspondingly). Xu *et al*. (2019) reported that the light-saturated P_N increased to the highest value about 10 d after leaf emergence (approximately the Top-2nd leaf correspondingly) and then decreased during leaf ontogeny at the jointing stage, which also indicated that light-saturated P_N increased at first and then decreased with lowering leaf position, as the new leaf emerged at the upper canopy.

The ratio of C_i to C_a decreased to the minimum for the Top-3rd leaf and then increased with lowering leaf position (Table 1), which was in contrast to the trend of P_N (Fig. 2). The decrease in P_N was commensurate with a marked increase in C_i as C_i decreased in intercellular spaces as a result of increased carbon fixation (Messinger *et al*. 2006). The C_{a1} and C_{a2} fell in the range of 311.3–610.8 μmol mol^{-1} and 884.6–1,291.4 μmol mol^{-1}, respectively. The atmospheric CO_2 concentration was about 400 μmol mol^{-1} (Zhang *et al*. 2019); this indicated the leaf P_N was limited by Rubisco activity or RuBP regeneration under field conditions. The results agreed with the neglectful TPU-limited photosynthesis for numerous leaf photosynthesis model (Chen *et al*. 1999, Yamori *et al*. 2011).

The V_{cmax}, J_{max}, and V_p in Fig. 3 indicated the photosynthesis capacity of rice leaf during Rubisco-limited, RuBP-limited, and TPU-limited stages in Fig. 2, and the high V_{cmax}, J_{max}, and V_p exhibited high leaf photosynthesis capacity (Long and Bernacchi 2003, Sharkey *et al*. 2007, Webster *et al*. 2016). The vertical profiles of J_{max} and V_p (Fig. 3*B*,*C*) were respectively clearly consistent with the variation in P_N during RuBP-limited and TPU-limited stages (Fig. 2), while the consistency of V_{cmax} (Fig. 3*A*) with P_N was unclear under low CO_2 concentration during the Rubisco-limited stage (Fig. 2), as the P_N was mainly affected by mitochondrial respiration. For V_{cmax}, J_{max}, and V_p, the variation in leaf nitrogen status might be an important trait in interpreting their profile within the rice canopy (Yamori *et al*. 2011). The potential photosynthetic capacity of rice leaf was highly related to leaf nitrogen content (Xu *et al*. 2014, Yang *et al*. 2016), and V_{cmax}, J_{max}, and V_p markedly increased with an increasing leaf nitrogen content (Nakano *et al*. 1997, Yin *et al*. 2009, Gu *et al*. 2012). Moreover, the leaf nitrogen content was low for the upper new-emerged and unexpanded leaf and usually decreased from the top to the bottom of rice canopy for the fully expanded leaf (Yang *et al*. 2014, Okami *et al*. 2016), which indicated the patterns of V_{cmax}, J_{max}, and V_p in Fig. 3*A–C*. Furthermore, the V_{cmax} was positively related to both the content and activity of Rubisco (Galmés *et al*. 2013) and the J_{max} (Chen *et al*. 1999), Rubisco content and activity in rice increased with leaf expanding and declined with leaf senescence (Suzuki *et al*. 2009, Wang *et al*. 2009), which also indicated the patterns of V_{cmax} and J_{max} in Fig. 3*A*,*B* as new rice leaves emerged at the upper canopy.

The ratios of J_{max} to V_{cmax} were 1.05, 1.19, 1.18, 1.22, 1.07, 1.10, and 1.04 for Top-1st, Top-2nd, Top-3rd, Top-4th, Top-5th, Top-6th, and Top-7th leaves (J_{max} and V_{cmax} were shown in Fig. 3), contrasting with current terrestrial biosphere models, in which J_{max} is usually calculated from the model-specific V_{cmax} input using a predetermined and constant ratio of J_{max} to V_{cmax} (Gu *et al*. 2010, Rogers *et al*.

2017). While the varied ratios of J_{max} to V_{cmax} agreed with the increasing research, the relationship between J_{max} and V_{cmax} varied with changed leaf attributes (Song *et al.* 2021). Moreover, the variation in ratios of J_{max} to V_{cmax} was also consistent with the C_{i1} (Table 1), as the increase in the ratios increased the CO_2 concentration at which the photosynthetic rate was co-limited by carboxylation and regeneration of RuBP (Onoda *et al*. 2005).

The decreased g_m with lowering leaf position was similar with decreased g_m with leaf age (Flexas *et al*. 2008), while was slightly different from positively correlated g_m with leaf nitrogen (Yamori *et al*. 2011). The vertical profiles of parameters in the FvCB model provided important evidence that foliage physiological characteristics varied greatly within crop canopy. Coupling this information with the vertical distribution of leaf attributes, microclimate, *etc*., within crop canopy will offer a theoretical method for upscaling leaf photosynthesis or their parameters to canopy scale.

References

Alagarswamy G., Boote K.J., Allen Jr. L.H., Jones J.W.: Evaluating the CROPGRO–soybean model ability to simulate photosynthesis response to carbon dioxide levels. – Agron. J. **98**: 34-42, 2006.

Bernacchi C.J., Bagley J.E., Serbin S.P. *et al*.: Modelling C_3 photosynthesis from the chloroplast to the ecosystem. – Plant Cell Environ. **36**: 1641-1657, 2013.

Busch F.A., Sage R.F., Farquhar G.D.: Plants increase CO_2 uptake by assimilating nitrogen via the photorespiratory pathway. – Nat. Plants **4**: 46-54, 2018.

Chen J.M., Liu J., Cihlar J., Goulden M.L.: Daily canopy photosynthesis model through temporal and spatial scaling for remote sensing applications. – Ecol. Model. **124**: 99-119, 1999.

de Pury D.G.G., Farquhar G.D.: Simple scaling of photosynthesis from leaves to canopies without the errors of big-leaf models. – Plant Cell Environ. **20**: 537-557, 1997.

Farquhar G.D., von Caemmerer S., Berry J.A.: A biochemical model of photosynthetic CO_2 assimilation in leaves of C_3 species. – Planta **149**: 78-90, 1980.

Flexas J., Ribas-Carbó M., Diaz-Espejo A. *et al*.: Mesophyll conductance to CO_2: current knowledge and future prospects. – Plant Cell Environ. **31**: 602-621, 2008.

Galmés J., Aranjuelo I., Medrano H., Flexas J.: Variation in Rubisco content and activity under variable climatic factors. – Photosynth. Res. **117**: 73-90, 2013.

Gong X.W., Li J., Ma H.C. *et al*.: Nitrogen deficiency induced a decrease in grain yield related to photosynthetic characteristics, carbon–nitrogen balance and nitrogen use efficiency in proso millet (*Panicum miliaceum* L.). – Arch. Agron. Soil Sci. **66**: 398-413, 2020.

Greer D.H., Weedon M.M.: Modelling photosynthetic responses to temperature of grapevine (*Vitis vinifera* cv. Semillon) leaves on vines grown in a hot climate. – Plant Cell Environ. **35**: 1050-1064, 2011.

Gu J.F., Yin X.Y., Stomph T.J. *et al*.: Physiological basis of genetic variation in leaf photosynthesis among rice (*Oryza sativa* L.) introgression lines under drought and well-watered conditions. – J. Exp. Bot. **63**: 5137-5153, 2012.

Gu L.H., Pallardy S.G., Tu K. *et al*.: Reliable estimation of biochemical parameters from C_3 leaf photosynthesis–intercellular carbon dioxide response curves. – Plant Cell Environ. **33**: 1852-1874, 2010.

Jin S.H., Wang P.M., Zhao K. *et al*.: Characteristic of gas exchange and chlorophyll fluorescence in different position leaves at booting stage in rice plants. – Rice Sci. **11**: 283-289, 2004.

Kattge J., Knorr W.: Temperature acclimation in a biochemical model of photosynthesis: a reanalysis of data from 36 species. – Plant Cell Environ. **30**: 1176-1190, 2007.

Kim J.H., Lee J.W., Ahn T.I. *et al*.: Sweet pepper (*Capsicum annuum* L.) canopy photosynthesis modeling using 3D plant architecture and light ray-tracing. – Front. Plant Sci. **7**: 1321, 2016.

Kim S.H., Lieth J.H.: A coupled model of photosynthesis, stomatal conductance and transpiration for a rose leaf (*Rosa hybrida* L.). – Ann. Bot.-London **91**: 771-781, 2003.

Li D.D., Tian M.Y., Cai J. *et al*.: Effects of low nitrogen supply on relationships between photosynthesis and nitrogen status at different leaf position in wheat seedlings. – Plant Growth Regul. **70**: 257-263, 2013.

Long S.P., Bernacchi C.J.: Gas exchange measurements, what can they tell us about the underlying limitations to photosynthesis? Procedures and sources of error. – J. Exp. Bot. **54**: 2393-2401, 2003.

Lv Y.P., Xu J.Z., Liu X.Y., Wang H.Y.: Vertical profile of photosynthetic light response within rice canopy. – Int. J. Biometeorol. **64**: 1699-1708, 2020.

Manter D.K., Kerrigan J.: A/C_i curve analysis across a range of woody plant species: influence of regression analysis parameters and mesophyll conductance. – J. Exp. Bot. **55**: 2581-2588, 2004.

Messinger S.M., Buckley T.N., Mott K.A.: Evidence for involvement of photosynthetic processes in the stomatal response to CO_2. – Plant Physiol. **140**: 771-778, 2006.

Nakano H., Makino A., Mae T.: The effect of elevated partial pressures of CO_2 on the relationship between photosynthetic capacity and N content in rice leaves. – Plant Physiol. **115**: 191-198, 1997.

Niinemets Ü.: Leaf age dependent changes in within-canopy variation in leaf functional traits: a meta-analysis. – J. Plant Res. **129**: 313-338, 2016.

Okami M., Kato Y., Yamagishi J.: Canopy architecture and leaf nitrogen distribution of rice (*Oryza sativa* L.) under chronic soil water deficit. – J. Agron. Crop Sci. **202**: 464-471, 2016.

Onoda Y., Hikosaka K., Hirose T.: Seasonal change in the balance between capacities of RuBP carboxylation and RuBP regeneration affects CO_2 response of photosynthesis in *Polygonum cuspidatum*. – J. Exp. Bot. **56**: 755-763, 2005.

Patrick L.D., Ogle K., Tissue D.T.: A hierarchical Bayesian approach for estimation of photosynthetic parameters of C_3 plants. – Plant Cell Environ. **32**: 1695-1709, 2009.

Peri P.L., Arena M., Martínez Pastur G., Lencinas M.V.: Photosynthetic response to different light intensities, water status and leaf age of two Berberis, species (Berberidaceae) of Patagonian steppe, Argentina. – J. Arid Environ. **75**: 1218-1222, 2011.

Pettersen R.I., Torre S., Gislerød H.R.: Effects of leaf aging and light duration on photosynthetic characteristics in a cucumber canopy. – Sci. Hortic.-Amsterdam **125**: 82-87, 2010.

Qian T., Elings A., Dieleman J.A. *et al*.: Estimation of photosynthesis parameters for a modified Farquhar–von Caemmerer–Berry model using simultaneous estimation method and nonlinear mixed effects model. – Environ. Exp. Bot. **82**: 66-73, 2012.

Ren B.Z., Li L.L., Dong S.T. *et al*.: Photosynthetic characteristics of summer maize hybrids with different plant heights. – Agron. J. **109**: 1454-1462, 2017.

Retkute R., Townsend A.J., Murchie E.H. *et al.*: Three-dimensional plant architecture and sunlit-shaded patterns: a stochastic model of light dynamics in canopies. – Ann. Bot.-London **122**: 291-302, 2018.

Rogers A., Serbin S.P., Ely K.S. *et al.*: Terrestrial biosphere models underestimate photosynthetic capacity and CO_2 assimilation in the Arctic. – New Phytol. **216**: 1090-1103, 2017.

Sharkey T.D., Bernacchi C.J., Farquhar G.D., Singsaas E.L.: Fitting photosynthetic carbon dioxide response curves for C_3 leaves. – Plant Cell Environ. **30**: 1035-1040, 2007.

Song G.M., Wang Q., Jin J.: Including leaf trait information helps empirical estimation of J_{max} from V_{cmax} in cool-temperate deciduous forests. – Plant Physiol. Bioch. **166**: 839-848, 2021.

Suzuki Y., Miyamoto T., Yoshizawa R. *et al.*: Rubisco content and photosynthesis of leaves at different positions in transgenic rice with an overexpression of *RBCS*. – Plant Cell Environ. **32**: 417-427, 2009.

Townsend A.J., Retkute R., Chinnathambi K. *et al.*: Suboptimal acclimation of photosynthesis to light in wheat canopies. – Plant Physiol. **176**: 1233-1246, 2018.

Walker A.P., Beckerman A.P., Gu L.H. *et al.*: The relationship of leaf photosynthetic traits – V_{cmax} and J_{max} – to leaf nitrogen, leaf phosphorus, and specific leaf area: a meta-analysis and modeling study. – Ecol. Evol. **4**: 3218-3235, 2014.

Wang C.J., Zhang Y.Q., Wang J.D. *et al.*: Plastic film mulching with drip irrigation promotes maize (*Zea mays* L.) yield and water-use efficiency by improving photosynthetic characteristics. – Arch. Agron. Soil Sci. **67**: 191-204, 2021.

Wang D., Lu Q., Li X.F. *et al.*: Relationship between Rubisco activase isoform levels and photosynthetic rate in different leaf positions of rice plant. – Photosynthetica **47**: 621-629, 2009.

Wang H.B., Ma M.G., Xie Y.M. *et al.*: Parameter inversion estimation in photosynthetic models: Impact of different simulation methods. – Photosynthetica **52**: 233-246, 2014.

Wang J., Wen X.F., Zhang X.Y. *et al.*: Co-regulation of photosynthetic capacity by nitrogen, phosphorus and magnesium in a subtropical Karst forest in China. – Sci. Rep.-UK **8**: 7406, 2018.

Wang X.P., Guo Y., Li B.G. *et al.*: Evaluating a three dimensional model of diffuse photosynthetically active radiation in maize canopies. – Int. J. Biometeorol. **50**: 349-357, 2006.

Webster R.J., Driever S.M., Kromdijk J. *et al.*: High C_3 photosynthetic capacity and high intrinsic water use efficiency underlies the high productivity of the bioenergy grass *Arundo donax*. – Sci. Rep.-UK **6**: 20694, 2016.

Wu A., Song Y.H., van Oosterom E.J., Hammer G.L.: Connecting biochemical photosynthesis models with crop models to support crop improvement. – Front. Plant Sci. **7**: 1518, 2016.

Xu J.Z., Lv Y.P., Liu X.Y. *et al.*: A general non-rectangular hyperbola equation for photosynthetic light response curve of rice at various leaf ages. – Sci. Rep.-UK **9**: 9909, 2019.

Xu J.Z., Yu Y.M., Peng S.Z. *et al.*: A modified nonrectangular hyperbola equation for photosynthetic light-response curves of leaves with different nitrogen status. – Photosynthetica **52**: 117-123, 2014.

Yamori W., Nagai T., Makino A.: The rate-limiting step for CO_2 assimilation at different temperatures is influenced by the leaf nitrogen content in several C_3 crop species. – Plant Cell Environ. **34**: 764-777, 2011.

Yang H., Li J.W., Yang J.P. *et al.*: Effects of nitrogen application rate and leaf age on the distribution pattern of leaf SPAD readings in the rice canopy. – PLoS ONE **9**: e88421, 2014.

Yang J., Gong W., Shi S. *et al.*: Estimation of nitrogen content based on fluorescence spectrum and principal component analysis in paddy rice. – Plant Cell Environ. **62**: 178-183, 2016.

Yin X.Y., Struik P.C., Romero P. *et al.*: Using combined measurements of gas exchange and chlorophyll fluorescence to estimate parameters of a biochemical C_3 photosynthesis model: A critical appraisal and a new integrated approach applied to leaves in a wheat (*Triticum aestivum*) canopy. – Plant Cell Environ. **32**: 448-464, 2009.

Zhang F.M., Chen J.M., Chen J.Q. *et al.*: Evaluating spatial and temporal patterns of MODIS GPP over the conterminous U.S. against flux measurements and a process model. – Remote Sens. Environ. **124**: 717-729, 2012.

Zhang Y.F., Yang P., Yang H. *et al.*: Plot-scale spatiotemporal variations of CO_2 concentration and flux across water–air interfaces at aquaculture shrimp ponds in a subtropical estuary. – Environ. Sci. Pollut. R. **26**: 5623-5637, 2019.

Zhang Y.G., Guanter L., Berry J.A. *et al.*: Estimation of vegetation photosynthetic capacity from space-based measurements of chlorophyll fluorescence for terrestrial biosphere models. – Glob. Change Biol. **20**: 3727-3742, 2014.

Zhang Y.G., Guanter L., Joiner J. *et al.*: Spatially-explicit monitoring of crop photosynthetic capacity through the use of space-based chlorophyll fluorescence data. – Remote Sens. Environ. **210**: 362-374, 2018.

Zhou Y.H., Lam H.M., Zhang J.H.: Inhibition of photosynthesis and energy dissipation induced by water and high light stresses in rice. – J. Exp. Bot. **58**: 1207-1217, 2007.